

## THERMODYNAMIC ANALYSIS OF FLUID FLOW IN CHANNELS WITH WAVY SINUSOIDAL WALLS

by

**Haitham M. S. BAH AidARAH and Ahmet Z. SAHIN \***

Mechanical Engineering Department, King Fahd University of Petroleum and Minerals,  
Dhahran, Saudi Arabia

Original scientific paper  
DOI: 10.2298/TSC1110403200B

*Entropy generation in channels with non-uniform cross-section that can be found in many fluid flow systems is an important concern from the thermodynamic design point of view. In this regard, the entropy generation in channels with periodic wavy sinusoidal walls has been considered in the present study. The flow is assumed to be 2-D steady laminar and the main parameters considered are the Reynolds number, height ratio  $H_{min}/H_{max}$  and module length ratio  $L/a$ . The fluid enters the channel with uniform axial velocity and temperature. The wall of the channel is assumed to be at uniform temperature which is different that of the fluid at the inlet of the channel. The distribution of the entropy generation as well as the total entropy generation has been studied numerically. It is found that the Reynolds number and the geometric parameters, height ratio and module length ratio have significant effect on both the local concentrations of entropy generation as well as the total entropy generation in the channel. Flow separation and re-circulation size, strength and location of flow are found to be major concern in determining the local entropy generation.*

Key words: *channel flow, entropy generation, heat transfer, sinusoidal wall*

### Introduction

Entropy generation has been the subject of investigation in many engineering applications for the purpose of improving the second law efficiency and providing sustainability. Since the entropy generation is related to not only the thermo-physical properties of materials but also the geometry of the thermal system, study of entropy generation is carried out on individual bases. It is known that any design modification made in a thermal system to enhance for example the heat transfer directly affects the entropy generation within the system. Among the many investigations that can be found in the literature in this regard, Sahin [1, 2] studied the effect of the cross-sectional geometry of a fluid flow duct on the entropy generation in an effort to minimize the entropy generation.

Heat transfer enhancement has been an extremely important consideration for heat exchanger applications that can be found in numerous engineering processes ranging from micro size medical to huge power plant systems. It is very common to use wavy channels to enhance the heat transfer in particularly compact heat exchangers. The fluid flow and heat transfer characteristics in wavy channel for the case of 2-D steady laminar fluid flow have been studied by Bahaidarah *et al.* [3]. The subject of the present work is to investigate the entropy generation

---

\* Corresponding author; e-mail: azsahin@kfupm.edu.sa

for the same geometry and study the effects of various geometric parameters of the wavy sinusoidal channel on the entropy generation.

The subject of heat transfer enhancement is extremely important for heat exchanger applications. Numerous publications have been devoted to the study of creative ways of increasing the heat transfer rate in compact heat exchangers [4]. The symmetric corrugated or wavy-walled channel is one of several devices utilized for enhancing the heat and mass transfer efficiency. The characteristics of the flow and heat transfer in a channel with such a configuration have been the subject of several investigations including Nishimure *et al.* [5], Nishimura *et al.* [6], Ali and Ramadhyani [7], Wang and Vanka [8], Stone and Vanka [9], and Niceno and Nobile [10]. However, none of these works have included the second law analysis or the entropy generation in the channel.

On the other hand entropy generation in channel flow has been studied by many researchers. Abbasi *et al.* [11] analyzed the entropy generation in Poiseuille-Benard channel flow with the use of the classic Boussinesq incompressible approximation. They found that the maximum entropy generation is localized at areas where heat exchanged between the walls and the flow is the maximum. They observed no significant entropy production in the main flow.

Haddad *et al.* [12] studied the entropy production due to laminar forced convection in the entrance region of a concentric cylindrical annulus. They found that the entropy generation is inversely proportional to both Reynolds number ( $Re$ ) and the dimensionless entrance temperature. They also observed that increasing Eckert number and/or the radius ratio will increase the entropy generation.

Ko and Cheng [13] investigated the developing laminar forced convection and entropy generation in a wavy channel. They considered the effects of aspect ratio ( $W/H$ ) and the Reynolds number on entropy generation. They found that the case of  $W/H = 1$  provided the minimal entropy generation. In addition, the higher  $Re$  is found to be beneficial for obtaining the lower values of the total resultant entropy generation in the flow field. Accordingly, the case with  $W/H = 1$  and higher  $Re$  is suggested to be used so that the irreversibility resulted from the developing laminar forced convection in the wavy channel could be the least. In another paper, Ko [14] studied the effects of corrugation angle on the developing laminar forced convection and entropy generation in a wavy channel. He analyzed flow characteristics including re-circulating flows, secondary vortices, temperature distributions, and friction factor as well as Nusselt number. He discussed the effects of corrugation angle on the distributions and magnitudes of local entropy generation resulted from frictional irreversibility and heat transfer irreversibility.

Heat transfer and fluid flow characteristics inside a wavy walled enclosure were studied numerically by Mahmud and Sadrul Islam [15]. They applied the second law of thermodynamics to predict the nature of irreversibility in terms of entropy generation. They carried out simulation for a range of wave ratio, aspect ratio and angle of inclination.

Mahmud and Fraser [16] studied the entropy generation inside a cavity made of two horizontal straight walls and two vertical wavy walls of sinusoidal shape for the case of laminar natural convection. In their analysis the horizontal straight walls are kept adiabatic, while the vertical wavy walls are isothermal but kept at different temperatures.

Ko [17] investigated numerically the entropy generation in a double-sine duct, which is frequently used in plate heat exchangers. He concluded that the entropy generation, in cases with larger  $Re$  and smaller heat transfer is dominated by the entropy generation due to frictional irreversibility; whereas the entropy generation is dominated by the entropy generation due to heat transfer irreversibility in cases with smaller  $Re$  and larger heat transfer.

The purpose of the present study is to examine the effects of geometric parameters on the 2-D developing fluid flow and heat transfer characteristics as well as the entropy generation in symmetric wavy channels and steady laminar flow. The flow is assumed to stay laminar and stable throughout the wavy channel, *i. e.* no bifurcations occur within the Re range considered in the present paper. Vortex instability and travelling wave instability that would normally occur for the case of high Re are not considered and can be found in other works such as refs. [18, 19].

### Geometric configurations

The geometric configuration considered is the sinusoidal channel as shown in fig. 1. The governing independent parameters influencing the fluid flow and heat transfer through a periodic array of wavy passage are the Re, height ratio ( $H_{\min}/H_{\max}$ ), and module length ratio ( $L/a$ ). Table 1 shows all configurations considered in this study. Each case is assigned a unique name and is studied for Re values of 25, 100, and 400.

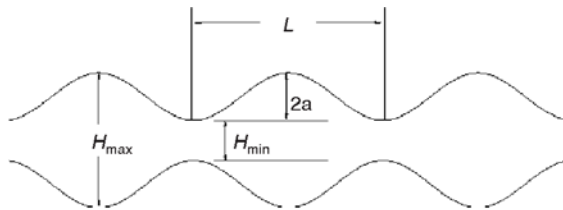


Figure 1. Periodic sinusoidal channel and the relevant parameters used in this study

Since the boundaries of the physical domain are irregular or represent complex geometries, a body-fitted grid or non-orthogonal grid system was developed to generate the grid for the domain of interest. The grids shown in fig. 2 were generated using algebraic grid-generation techniques. The physical domains illustrated in fig. 1 can be discretized using the algebraic sheared transformation. The x co-ordinate was discretized into equally spaced points. The y co-ordinate was discretized into equally spaced points at each x location by the normalizing transformation technique as:

$$y = \left( \frac{\eta - 1}{\eta_{\max} - 1} \right) Y(x) \quad 1 \leq \eta \leq \eta_{\max} \quad (1)$$

where  $Y(x)$  is the upper boundary, which is the sine function for the sinusoidal shaped channel. This kind of grid-generation technique produces regular or structured grids. The reader is referred to Hoffman [20] for further details.

The computational domain is divided into three individual regions. Those regions are the entry region, the periodic wavy modules, and the exit region. A uniform orthogonal grid is used for both the entry and exit regions. The grid distribution shown in fig. 2 can be repeated successively to generate the domain of periodic wavy modules. In this study, six consecutive

Table 1. Parameters used in the sinusoidal configuration

Configuration	$L/a$	$H_{\min}/H_{\max}$
L-4-H-3	4	0.3
L-4-H-5	4	0.5
L-4-H-7	4	0.7
L-8-H-3	8	0.3
L-8-H-5	8	0.5
L-8-H-7	8	0.7
L-16-H-3	16	0.3
L-16-H-5	16	0.5
L-16-H-7	16	0.7

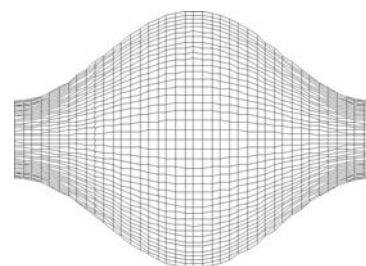


Figure 2. Grid distributions for one module of wavy sine-shaped channel

modules are included in the computational domain. The scalar and velocity variables are stored at staggered grid locations. All thermo-physical properties are stored at the main grid locations, while the velocity variables are stored at the interface of each control volume.

### Mathematical formulation

Consider the 2-D periodic sinusoidal cross-sectional channel, as shown in fig. 1. The thickness of the channel is neglected and the thermal boundary condition on the surface of the channel is assumed to be uniform wall temperature  $T_w$ . Fluid enters the channel with uniform axial velocity  $u = U_{in}$  and uniform temperature  $T_{in}$ . Both hydrodynamic and thermal boundary layers start developing. The purpose is to study the volumetric entropy generation rate distribution throughout the fluid in the channel. This requires solution of velocity and temperature fields in the fluid. The governing equations and the boundary conditions for this steady problem are [21]:

– continuity

$$\frac{\partial u}{\partial x} + \frac{\partial v}{\partial y} = 0 \quad (2)$$

– momentum

$$u \frac{\partial u}{\partial x} + v \frac{\partial u}{\partial y} = -\frac{1}{\rho} \frac{\partial p}{\partial x} + \frac{\mu}{\rho} \left( \frac{\partial^2 u}{\partial x^2} + \frac{\partial^2 u}{\partial y^2} \right) \quad (3)$$

$$u \frac{\partial v}{\partial x} + v \frac{\partial v}{\partial y} = -\frac{1}{\rho} \frac{\partial p}{\partial y} + \frac{\mu}{\rho} \left( \frac{\partial^2 v}{\partial x^2} + \frac{\partial^2 v}{\partial y^2} \right) \quad (4)$$

– energy

$$\rho C_p \left( u \frac{\partial T}{\partial x} + v \frac{\partial T}{\partial y} \right) = k \left( \frac{\partial^2 T}{\partial x^2} + \frac{\partial^2 T}{\partial y^2} \right) + \mu \Phi \quad (5)$$

– entropy generation rate

$$\dot{S}_{gen}''' = \frac{k}{T^2} \left[ \left( \frac{\partial T}{\partial x} \right)^2 + \left( \frac{\partial T}{\partial y} \right)^2 \right] + \frac{\mu}{T} \Phi \quad (6)$$

where the dissipation function  $\Phi$  is given by:

$$\Phi = 2 \left[ \left( \frac{\partial u}{\partial x} \right)^2 + \left( \frac{\partial v}{\partial y} \right)^2 \right] + \left( \frac{\partial u}{\partial y} + \frac{\partial v}{\partial x} \right)^2 \quad (7)$$

The first term in eq. (6) represents the entropy generation due to heat conduction in the radial and axial directions. The last term, on the other hand, accounts for the fluid friction contribution to the entropy generation.

### Boundary conditions

A no-slip boundary condition was assigned at the walls, where both velocity components are set to zero (*e. g.*,  $u = v = 0$ ). The channel was subjected to a constant wall temperature ( $T = T_w$ ) condition. A uniform inlet velocity profile was assigned at the inlet boundary condition ( $u = U_{in}$ ). A constant inlet temperature ( $T = T_{in}$ ), different than the wall temperature, was assigned at the channel inlet. The streamwise gradients of all variables were set to zero at the outlet boundary to attain a fully developed state in which no change takes place in the flow direction.

### Convergence criteria

The discretization equations obtained by integrating the governing partial differential equations resulted in a set of linear algebraic equations for each variable which need to be solved iteratively. The set of linear algebraic equations were solved sequentially within each iteration. A set of these equations was solved by using the line-by-line method, which is a combination of the tridiagonal matrix algorithm and the Gauss-Siedel procedure. Convergence could be declared if the maximum of the absolute value of the mass residues was less than a very small number  $\varepsilon$  (e. g.,  $10^{-5}$ ). In this study, convergence was declared by monitoring the sum of the residues at each node. Since the magnitude of  $u_\xi$  and  $u_\eta$  are not known *a priori*, monitoring the relative residuals is more meaningful. The relative convergence criteria for  $u_\xi$  and  $u_\eta$  are defined as:

$$\bar{R}_{u_\xi} = \frac{\sum_{\text{nodes}} |a_e u_{\xi,e} - \sum a_{nb} u_{\xi,nb} - b_{u_{NO}} - A_e (P_P - P_E)|}{\sum_{\text{nodes}} |a_e u_{\xi,e}|} \leq \varepsilon_{u_\xi} \quad (8)$$

$$\bar{R}_{u_\eta} = \frac{\sum_{\text{nodes}} |a_n u_{\eta,n} - \sum a_{nb} u_{\eta,nb} - b_{u_{NO}} - A_n (P_P - P_N)|}{\sum_{\text{nodes}} |a_n u_{\eta,n}|} \leq \varepsilon_{u_\eta} \quad (9)$$

In the pressure equation, it is appropriate to check for mass imbalance in the continuity equation. The convergence criterion for pressure was defined as:

$$R_p = \sum_{\text{nodes}} |b + b_{NO}| \leq \varepsilon_p \quad (10)$$

The convergence criterion for temperature was defined as:

$$R_T = \sum_{\text{nodes}} |b_p T_p - \sum a_{nb} T_{nb} - b_{T,NO}| \leq \varepsilon_p \quad (11)$$

The numerical iteration criterion required that the normalized residuals of mass, momentum, and energy be less than  $10^{-6}$  for all cases considered in this study.

### Validations

The developed code was validated by reproducing solutions for some benchmark problems. The fluid flow and heat transfer in a parallel-plate channel subjected to constant wall temperature was predicted. As expected from classical results for this problem, the flow will develop in the entrance region until it reaches fully developed condition, at which no further changes in velocity profile take place in the streamwise direction. Since the gradient of pressure in the fully developed region is constant, the velocity profile is parabolic, with the point of maximum velocity located along the centerline and equal to 1.5 times the mean velocity. The Nusselt number (Nu) for the fully developed region between two parallel plates subjected to constant wall temperature is 7.56, which agrees favorably with the Nu 7.54 mentioned by many authors, such as Incropera and DeWitt [22].

As mentioned earlier, Wang and Vanka [8] studied numerically the 2-D steady and time-dependent fluid flow and heat transfer through a periodic sinusoidal-shaped channel for fluid with a Prandtl number of 0.7 for one set of geometric parameters,  $H_{\min}/H_{\max} = 0.3$  and  $L/a = 8$ . They presented a comparison of the calculated separation and re-attachment points with the experimental data of Nishimura *et al.* [6]. They also presented the Nu distribution along the walls of the sine-shaped channel. Figure 3 shows the local Nu presented by Wang and Vanka [8] for a single periodically fully developed (PDF) module and the developing flow results generated in the present work for six consecutive modules. Disregarding the first module, the next five modules show

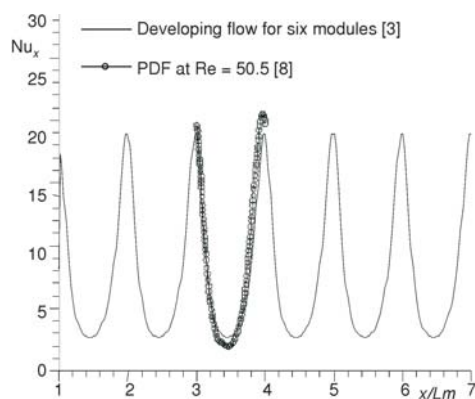


Figure 3. Local Nusselt number along the walls of a sine-shaped channel

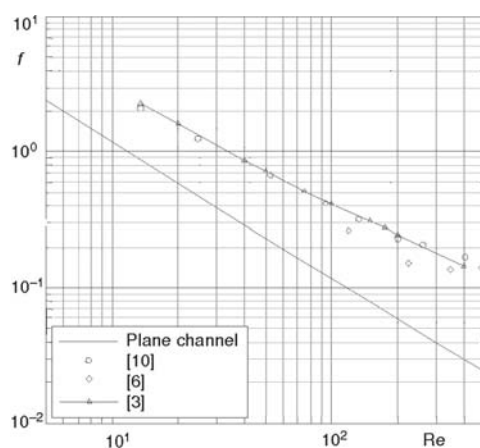


Figure 4. Friction factor for the fourth module of a sine-shaped channel

$$f = \frac{[P_m(MI) - P_m(MO)]H_{av}}{(L)(2\rho u_{av}^2)} \quad (13)$$

where  $MI$  and  $MO$  stand for module inlet and module outlet, respectively,  $P_m$  is the mean pressure,  $H_{av}$  – the average channel height ( $H_{av} = H_{max}/2 + H_{min}/2$ ), and  $u_{av}$  – the average velocity in a single module in the channel. The  $Re$  is defined as:

$$Re = \frac{\rho u_{av} H_{av}}{\mu} \quad (14)$$

### Grid independence

Structured symmetric grids were used for the computations to ensure symmetric solutions. A grid refinement study was performed in order to assess the accuracy of the results. Table 2 gives a summary of the grid independence test for both sine-shaped and arc-shaped channels at different  $Re$ . It can be seen from the results that the values of friction factor ( $f$ ) and  $Nu$  obtained

that the flow has reached the fully developed condition as they have the same behavior and the results of a PDF can fit to any one of them. The local  $Nu$  is given by:

$$Nu_x = \frac{2H_{av}}{T_w - T_{b,i}} \left. \frac{\partial T}{\partial y} \right|_{wall} \quad (12)$$

Niceno and Nobile [10] studied numerically the same flow problem by means of an unstructured co-volume method for the same set of geometric parameters, but for two different geometric configurations, *i. e.*, sinusoidal-shaped and arc-shaped channels. The flow and temperature fields were studied under the assumption of fully developed flow, which means that the flow repeats itself from module to module, and the heat transfer coefficient has reached its asymptotic value. Based on this assumption, Niceno and Nobile [10] analyzed only one module of the geometry. However, in this work, six consecutive modules were considered. The fully developed condition could be reached at the second or the third module and the results are comparable to those of Niceno and Nobile [10]. Figure 4 shows the results of the friction factors ( $f$ ) obtained for sine-shaped geometry for the fourth module as a function of  $Re$ . The result obtained with the developed code agrees with the numerical results of Niceno and Nobile [10] and the experimental observations of Nishimura *et al.* [6]. The friction factor was computed based on its standard definition:



at different grids vary by less than 1.8%, thus demonstrating the adequacy of the grid adopted and the numerical accuracy of the method. All calculations presented here were obtained with the finest grid (6,561 grid points).

**Table 2. Grid independence study**

		Grid 1 (1,681 grid points)	Grid 2 (3,721 grid points)	Grid 3 (6,561 grid points)
Re = 100	$f$	0.4153	0.4124	0.4115
	Nu	9.176	9.1527	9.1463
Re = 150	$f$	0.3096	0.3039	0.3010
	Nu	9.4428	9.3689	9.3355

### Results and discussion

The computational domain consists of six modules of sinusoidal shape wavy channel. The effect of Re,  $H_{\min}/H_{\max}$ , and  $L/a$  on the local as well as total entropy generation is discussed. The effect of each of these parameters on the velocity profile, streamline, normalized temperature field, normalized pressure drop, and module average Nu indicated that in most of the cases considered periodically fully developed profiles are attained downstream of the first two or three modules [3]. Thus, one module (the fourth module from the inlet) has been selected as a representative module to discuss the details of entropy generation.

The streamlines in the fourth module from the inlet are shown in fig. 5 for fixed height ratio  $H_{\min}/H_{\max} = 0.3$  and module length ratio  $L/a = 8$ . As Re is increased the flow separation and circulation increases and moves towards the exit of the module. This indicates that the velocity gradients attain greater values and their position moves as the Re is increased. For low Re (Re = 25) the circulation ceases and no separation is observed. In all cases the flow symmetry is observed as a result of symmetrical geometric configuration.

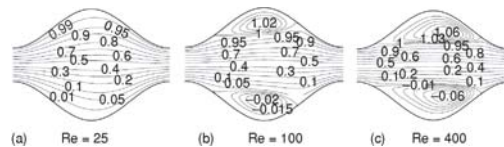


**Figure 5. Effect of Re on the streamlines for sinusoidal channel configuration, fourth module,  $H_{\min}/H_{\max} = 0.3$  and  $L/a = 8$**

For the case of low Re the velocity gradients are maximum at the inlet and exit locations where the cross-sectional areas are minimum. For larger Re, however, larger velocity gradients may be obtained within the module away from the inlet and exit locations as a result of the flow detachment and re-circulation.

The effect of Re on the temperature variation within the fourth module is shown in fig. 7. Dimensionless isotherms are shown for fixed height ratio  $H_{\min}/H_{\max} = 0.3$  and module length ratio  $L/a = 8$ . For low Re the temperature gradients are concentrated around the inlet region. In most of the remaining domain the gradients are small. As the Re is increased however the temperature gradients increase in the whole domain except along the flow centerline where the gradients are minimal as a result of insufficient time for the temperature penetration. Next to this centerline region the temperature gradients are relatively high. Temperature gradients along the surface of the channel near the exit location also increase as the Re is increased.

The velocity and temperature gradients shown in figs. 5 and 6 indicate the location and the strength of the entropy generation in the module. The variation of the entropy generation in the fourth module for the same height ratio and module length ratio as given in those figures is shown in fig. 7. As can be seen from fig. 7(a), the entropy generation in the entire domain is very

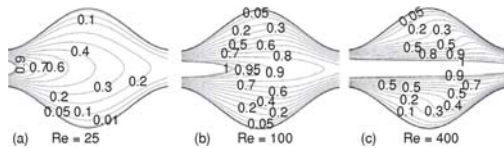


**Figure 6. Effect of Re on the isotherms for sinusoidal channel configuration, fourth module,  $H_{\min}/H_{\max} = 0.3$  and  $L/a = 8$**

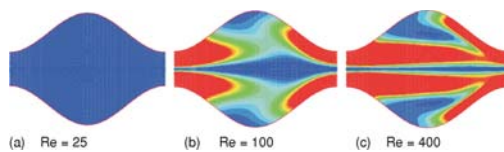


**Figure 7. Contour plots of entropy generation for fourth module,  $H_{\min}/H_{\max} = 0.3$  and  $L/a = 8$  (for color image see journal web site)**

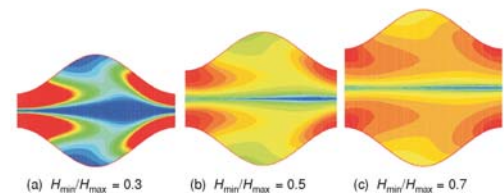


**Figure 8. Contour plots of entropy generation fourth module,  $L/a = 8$  and  $Re = 100$  (for color image see journal web site)**

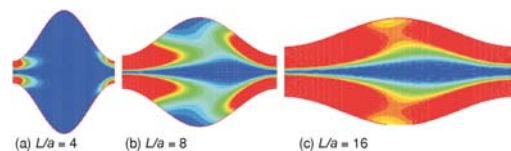


**Figure 9. Contour plots of entropy generation for fourth module,  $H_{\min}/H_{\max} = 0.3$  and  $Re = 100$  (for color image see journal web site)**

is concentrated in the regions close to the inlet and exit regions. This is due to the increase of the internal volume of the module and decrease of the velocity gradients within the module. Thermal and velocity gradients in this case occur around the inlet and exit locations where the flow cross-section is the minimum. On the other hand, when the length ratio is increased the entropy generation within the module volume increases in most parts of the domain except along the axis where the fluid flow attains high speed with smaller velocity gradients. The maximum entropy generation is observed along the wall surface of the channel with the exception of the location upstream of the region where flow separation and recirculation is observed. It should be noted that in the limit where the height ratio approaches infinity, the channel geometry approaches to that of straight channel in which the entropy generation will be concentrated near the channel wall and will seize along the centerline of the channel.

small and uniform. There are no concentrations of the entropy generation is observed. This is due to the uniform distribution of the velocity gradients with no flow separation and re-circulation and low temperature gradients. As the Re is increased the entropy generation rate around the inlet and exit locations increase, figs. 7(b) and 7(c). Along the centerline, the entropy generation is minimum within a certain region of flow thickness depending of the Re. This region of flow thickness decreases as the Re is increased. It should be also noted that there is a region of low entropy generation in both sides of the channel near the wall where the cross-section is large. This is due to the low velocity and temperature gradients due to the flow re-circulation activity taking place further downstream. As the Re is increased further, the concentration of the entropy generation increases around the thin centerline fluid jet and near the wall of the channel around the exit location. The symmetrical distribution of the entropy generation is also noted.

The geometric parameters, namely the height ratio  $H_{\min}/H_{\max}$  and module length ratio  $L/a$ , have a considerable influence on the distribution of entropy generation. Figure 8 shows the effect of the height ratio  $H_{\min}/H_{\max}$  on the entropy generation in the channel. As the height ratio is increased the distribution of the entropy generation increases and becomes more uniform throughout the major part of the domain.

Figure 9 shows the effect of the length ratio on the distribution of the entropy generation. For lower length ratio, the entropy generation



## Conclusions

Entropy generation in a channel with periodic sinusoidal wall is considered in the present study. The flow is considered to be laminar and the thermal boundary condition is assumed to be uniform temperature. The conclusions obtained from the present work can be summarized as follows.

The fluid attains a steady periodic laminar flow after a developing region that extends through one or two modular segments of the channel.

Re has a considerable effect on the local and overall entropy generation rate in the channel. In general, the entropy generation rate is concentrated around the inlet and the outlet sections of the periodic modules of the channel. As the Re increases flow separation and re-circulation occurs in the module resulting in local concentrations of the entropy generation within the channel.

The height ratio of the channel mainly affects the distribution of the entropy generation in the channel module. As the height ratio is increased the distribution of the entropy generation becomes more uniform in axial direction. Entropy generation rate in the transversal direction shows considerable fluctuations whose magnitude depends on the strength of the re-circulation of fluid flow in the module.

The module length ratio also affects the distribution of the entropy generation rate in the module volume, although the effect of it on the overall entropy generation is minimal. As the length ratio is decreased the re-circulation of fluid flow increases causing higher concentrations of local entropy generation in the channel module.

The distribution of the entropy generation rate in the wavy sinusoidal channel becomes important in designing the geometric configuration of fluid flow passages used in many engineering devices such as compact heat exchangers.

## Acknowledgment

The authors acknowledge the support provided by King Fahd University of Petroleum and Minerals, Dhahran, Saudi Arabia, for this work.

## Nomenclature

$A$	– area of heat transfer surfaces in a modulus, [m <sup>2</sup> ]
$a$	– coefficients
$b$	– source term
$C_p$	– specific heat, [Jkg <sup>-1</sup> K <sup>-1</sup> ]
$H$	– height, [m]
$h$	– heat transfer coefficient, [Wm <sup>2</sup> K <sup>-1</sup> ]
$k$	– thermal conductivity, [Wm <sup>-1</sup> K <sup>-1</sup> ]
$L$	– length, [m]
Nu	– Nusselt number (= $hH/k$ ), [-]
$P$	– pressure, [Pa]
$R$	– residue
Re	– Reynolds number (= $\rho uH/\mu$ ), [-]
$S$	– entropy, [kJkg <sup>-1</sup> K <sup>-1</sup> ]
$T$	– temperature, [K]
$u, v$	– Cartesian velocity components, [ms <sup>-1</sup> ]
$W$	– width, [m]
$x, y$	– Cartesian co-ordinates, [m]

## Greek symbols

$\varepsilon$	– convergence criteriam
$\eta, \xi$	– contravariant components of velocity, [ms <sup>-1</sup> ]
$\mu$	– viscosity, [Nsm <sup>-2</sup> ]
$\rho$	– density, [kgm <sup>-3</sup> ]

## Subscripts

av	– average
b	– bulk
E, N	– adjacent points to the main point P
e, w,	– adjacent faces to the main
n, s	point P
i	– module number
in	– inlet
nb	– neighboring points
NO	– non-orthogonal
w	– wall

## References

- [1] Sahin, A. Z., A Second Law Comparison for Optimum Shape of Duct Subjected to Constant Wall Temperature and Laminar Flow, *Heat and Mass Transfer*, 33 (1998), 5-6, pp. 425-430
- [2] Sahin, A. Z., Irreversibilities in Various Duct Geometries with Constant Wall Heat Flow and Laminar Flow, *Energy*, 23 (1998), 6, pp. 465-473
- [3] Bahaidarah, H. M. S., et al., Numerical Study of Heat and Momentum Transfer in Channels with Wavy Walls, *Numerical Heat Transfer, Part A*, 47 (2005), 5, pp. 417-439
- [4] \*\*, *Handbook of Single Phase Convective Heat Transfer* (Eds. S. Kakac, R. K. Shah, W. Aung), John Wiley and Sons, New York, USA, 1980, pp. 17.1-17.62
- [5] Nishimura, T., et al., Flow Characteristics in a Channel with Symmetric Wavy Wall for Steady Flow, *Journal of Chemical Engineering*, 17 (1984), 5, pp. 446-471
- [6] Nishimura, T., et al., Flow Observation and Mass Transfer Characteristics in Symmetrical Wavy-Walled Channels at Moderate Reynolds Numbers for Steady Flow, *International Journal of Heat and Mass Transfer*, 33 (1990), 5, pp. 835-845
- [7] Ali, M. M., Ramadhani, S., Experiments on Convective Heat Transfer in Corrugated Channels, *Experimental Heat Transfer*, 5 (1992), 3, pp. 175-193
- [8] Wang, G., Vanka, S. P., Convective Heat Transfer in Wavy Passage, *International Journal of Heat and Mass Transfer*, 38 (1995), 17, pp. 3219-3230
- [9] Stone, K., Vanka, S. P., Numerical Study of Developing Flow and Heat Transfer in a Wavy Passage, *Journal of Fluid Engineering*, 121 (1999), 4, pp. 713-719
- [10] Niceno, B., Nobile, E., Numerical Analysis of Fluid Flow and Heat Transfer in Periodic Wavy Channel, *International Journal of Heat and Fluid Flow*, 22 (2001), 2, pp. 156-167
- [11] Abbassi, H., et al., Entropy Generation in Poiseuille-Benard Channel Flow, *International Journal of Thermal Sciences*, 42 (2003), 12, pp. 1081-1088
- [12] Haddad, O. M., et al., Entropy Generation Due to Laminar Forced Convection in the Entrance Region of a Concentric Annulus, *Energy*, 29 (2004), 1, pp. 35-55
- [13] Ko, T. H., Cheng, C. S., Numerical Investigation on Developing Laminar Forced Convection and Entropy Generation in a Wavy Channel, *International Communications in Heat and Mass Transfer*, 34 (2007), 8, pp. 924-933
- [14] Ko, T. H., Effects of Corrugation Angle on Developing Laminar Forced Convection and Entropy Generation in a Wavy Channel, *Heat and Mass Transfer*, 44 (2007), 2, pp. 261-271
- [15] Mahmud, S., Sadrul Islam, A. K. M., Laminar Free Convection and Entropy Generation Inside an Inclined Wavy Enclosure, *International Journal of Thermal Sciences*, 42 (2003), 11, pp. 1003-1012
- [16] Mahmud, S., Fraser, R. A., Free Convection and Entropy Generation Inside a Vertical In-Phase Wavy Cavity, *International Communications in Heat and Mass Transfer*, 31 (2004), 4, pp. 455-566
- [17] Ko, T. H., Numerical Analysis of Entropy Generation and Optimal Reynolds Number for Developing Laminar Forced Convection in Double-Sine Ducts with Various Aspect Ratios, *International Journal of Heat and Mass Transfer*, 49 (2006), 3-4, pp. 718-726
- [18] Floryan, J. M., Vortex Instability in a Converging-Diverging Channel, *Journal of Fluid Mechanics*, 482 (2003), 5, pp. 17-50
- [19] Floryan, J. M., Floryan, C., Travelling Wave Instability in a Diverging-Converging Channel, *Fluid Dynamics Research*, 42 (2010), 2, pp. 025509-025529
- [20] Hoffman, J. D., *Numerical Methods for Engineers and Scientists*, McGraw-Hill, New York, USA, 1992
- [21] Arpaci, V. S., Larsen, P. S., *Convection Heat Transfer*, Prentice Hall, Englewood Cliffs, N. J., USA, 1984
- [22] Incropera, F. P., DeWitt, D. P., *Fundamentals of Heat and Mass Transfer*, John Wiley and Sons, New York, USA, 1996

Paper submitted: March 16, 2011

Paper revised: April 19, 2012

Paper accepted: May 4, 2012